Luminescence Studies of $(Zns)_{1-x}(Mnte)_x$ Nanophosphors Prepared by Wet Chemical Method

Dr Deepti Pateria
School of Studies in Physics and Astrophysics,
Pt. RaviShankar Shukla University,
Raipur-492010 (C.G.), India

Dr Prabhakar Pateria
Department of Chemistry
G.D. Rungta College of Engineering & Technology,
Bhilai (C.G.)

Abstract **- The present paper reports the luminescence behavior of $(ZnS)_{1-x}(MnTe)_x$ nanophosphors prepared by wet chemical synthesis. $(ZnS)_{1-x}(MnTe)_x$ nanophosphors give intense mechanoluminescence ,thermoluminescenceas as well photoluminescence. The structure investigated by X-ray diffraction patterns confirms the formation of sphalerite phase whose space group is found to be $F\bar{4}3$ m. From XRD measurement average size of particles was found of 11 nm. The TEM measurement indicates that the particle size is in the 9-13 nm. Nanometre size phosphors are preferred in a number of applications not only due to their particle size but also due to smooth imaging of the stress. As the PL, ML, and TL intensity of $(ZnS)_{1-x}(MnTe)_x$ phosphor is much higher as compared to ZnS: Mn phosphor, it can be used in lots of application like in biology, medicine, photonics and optoelectronics appear, damage sensor for structures ,ML based structural health monitoring, in various thermoluminescence applications like dosimeter etc. systems where ZnS:Mn phosphor is used presently. However, for higher values of x the luminescence intensity decreases because of the concentration quenching. Thus the Thermoluminescence (TL), Mechanoluminescence (ML) and Photoluminescence (PL) intensities are optimum for a particular value of x, that is, for x=0.05.**

Keywords –Luminescence, $(ZnS)_{1-x}(MnTe)_x$, Nanophosphors , Wet chemical method, II-IV semiconductors.

1. INTRODUCTION

Luminescence is the non-equilibrium phenomenon of excess emission over and above the thermal emission of a body, in which emission has a duration considerably exceeding the period of light oscillations. Although excess emission over and above the thermal background takes place in reflected and refracted light, Rayleigh and Raman scattering, and Cherenkov and laser radiations, they are not the phenomenon of luminescence as the emission duration in these phenomenon are of the order of the period of light oscillations. Whereas the intensity of incandescent emission increases with temperature, in most cases, the intensity of luminescence decreases with increasing temperature of materials. Luminescence may occur in crystalline and non-crystalline solids as well as in liquids and gases. Luminescence process involves at least three steps; (1) Energy absorption causing electronic excitation, (2) Storage of absorption energy and, (3) Emission of photon. Depending on the storage time, i.e., the time delay between the excitation and emission, luminescence can be classified in two categories. If the storage time is shorter than 10^{-8} sec, the process is termed as fluorescence, otherwise, it is phosphorescence. The interval 10^{-8} sec is chosen as it gives the lifetime of an atom in the excited stage, for which return to the ground state is accompanied by dipole radiation. [1-5].

Last two decades the luminescence of II-VI nanomaterials is attracting the interest of many workers [6]. Although photoluminescence [6-11] and electroluminescence [6,12-14] and mechanoluminescence [6, 15-17] of II-VI of semiconductors have been studied in detail, least studies on their TL have been made.Chen et al. [18, 19] have studied thermoluminescence of ZnS nanoparticles and they have reported that the TL intensity increases as the particle size is decreased. The significance of the present study are as follows (i) $(ZnS)_{1-x}(MnTe)_x$ nanophosphors prepared by wet chemical synthesis give intense mechanoluminescence ,thermoluminescenceas, as well as photoluminescence.,(ii)the luminescence intensity of (ZnS)1_x(MnTe)x nanophosphor prepared by a wet chemical method is very high nearly 5 times more as compared to that of ZnS: Mn phosphor. Therefore, such phosphor may replace ZnS:Mn phosphor in its use in damage sensor and mechanoluminescence structure health monitoring system, and (iii) the nano metre size phosphors are preferred in a number of applications not only due to their particle size but also for smooth imaging of the stress distribution in solids. Thus, the present study provides a sufficient novel knowledge which are quite unknown till now. As the PL, ML, and TL intensity of $(ZnS)_{1-x}(MnTe)_x$ phosphor is much higher as compared to ZnS: Mn phosphor, it can be used in lots of application like in biology, medicine, photonics and optoelectronics appear, damage sensor for structures ,ML based structural health monitoring, in various thermoluminescence applications like dosimeter etc. systems where ZnS:Mn phosphor is used presently.

The present paper reports the luminescence studies of $(ZnS)_{1-x}(MnTe)_x$ nanophosphors prepared by wet chemical method.

.

2. EXPERIMENTAL

For the present investigation the $(ZnS)_{1-x}(MnTe)_x$ nanophosphors were synthesized by wet chemical process. In the synthesis of $(ZnS)_{1-x}(MnTe)_x$ we used

$Zn(CH_3COO)_2.2H_2O$ (A.R. Himedia Laboratories., 99.5%), $Mn(CH_3COO)_2.4H_2O$ (AR fine-chem Limited., 99.5%), Na_2S9H_2O (Flakes, Himedia Laboratories Pvt. Ltd.) and TeO_2 (Himedia Laboratories Pvt. Ltd.97.0%) as the starting materials. Firstly, a certain molar proposition of Zn $(CH_3COO)_2.2H_2O$ and Mn $(CH_3COO)_2.4H_2O$ (Mn/Zn molar ratio = 5%) were dissolved in distilled water at room temperature with continuous stirring (solution 1). Similarly, $Na_2S.9H_2O$ and TeO_2 (Te/S molar ratio= 5%) were dissolved in distilled water with continuous stirring (solution 2). Then solution 1 and solution 2 were mixed together with continuous stirring whereby we found the precipitates of the material. Then the resulting precipitates were washed with distilled water many times. After the washing we separated the precipitates by centrifugation and then the precipitates were dried in vacuum. Finally, the dried precipitates were mixed with activated charcoal, and then the precipitates were fired at 850° C for 10 h. The powder phosphor obtained was used for the TL measurements.

The crystal-structure was determined by X-ray diffraction (XRD) (Buker D_2-Phaser) analysis using Cu $K\alpha$ radiation (λ=1.54 Å and 2θ= 20^0-70^0) at room temperature. A spectrofluorometer (Shimadzu Spectroflurophotometer RF 5301PC) was used for photoluminescence (PL) measurement at room temperature. In the present investigation ML in $(ZnS)_{1-x}(MnTe)_x$ phosphors was excited using impulsive technique. The phosphors were used without any irradiation such as UV, X-ray, γ rays, etc. In this experiment, inside the sample holder there is a transparent Lucite plate below the guiding cylinder. The sample of 4 mg was placed on the upper surface of the lucide plate. Then the sample was covered with a thin aluminums foil then it fixed using an adhesive tape. So it prevents the scattering of crystallite fragments while the impact of the load or piston onto the sample is applied. The ML was induced impulsively by applying a load onto the sample from a fixed height. By using RCA-931A photomultiplier tube (PMT) which placed just below the Lucite plate the luminescence intensity was measured.The themoluminescence measuring equipment is known as TLD reader. The experimental set up used for the present study was consists of a built-in arrangement for heating the sample, a photomultiplier tube, a high voltage power supply, a computer and a computer programme to read the TL glow curve.For the TL measurement the samples of 4 mg each were exposed to UV- light for different times such as 10 min, 25 min, and 20 min, 15 min. Then the sample was heated at a fixed heating rate of 10^0C per sec. Photomultiplier tube was used to detect individual emitted photons. The photomultiplier was preceded by optical filters to select the wavelength range of interest from the particular sample material. A microcomputer controls the heating rate and highest heating temperature and collects the data from room temperature up to 500^0 C. Heater strip can be programmed to heat the sample from 1^0 C/sec up to 40^0 C /sec and a maximum temperature that can be attained was (allowed) 500^0 C. One heat absorbing glass and IR cut off filter was used, which allows only visible light and cuts-off IR radiation.

3. RESULTS

Fig. 1 shows the XRD obtained in the present work for $(ZnS)_{1-x}(MnTe)_x$ powder samples. From this figure it is obvious that samples of all the compositions are polycrystalline in nature. The peaks of these XRDs for all samples are indexed using the standard ASTM Table and JCPDF data. In the present work all the samples were found to be in spheralite structure haveing space group were $F\bar{4}3$ m .Rao et al. [24, 25] have reported wurtzite structure while Toriyi et al. [26] have reported spheralite and wurtzite structure for ZnSMnTe system.

The XRD spectra of $(ZnS)_{1-x}(MnTe)_x$ powder samples exhibit sharp peaks at 2θ values equal to 28.91^0, 33.90^0, 48.11^0, 57.10^0, 59.89^0, 70.40^0, 77.83^0, 80.25^0 , 89.82^0 ,96.98^0, and 96.98^0, which correspond to diffraction from (111), (200), (220), (311), (222), (400), (331), (420), (422), and (333) planes, respectively. It can be very clearly seen from Fig 1 that the XRD pattern shows broadening in the peak. Nanomaterials have small particle size and this causes broadening in their diffraction peak. The broadening of the peak is due to a small number of crystal planes. The broadening in turn causes a loss of intensity in the signal of their diffraction patterns. Strain factors as well as broadening due to the instrument could also contribute to the broadening of the peaks. The average crystallite size was calculated using the Scherer's formula which gave the average particle size 11 nm. The lattice parameter has been computed as to be 5.34 Å.

Fig2 (a,b) show the TEM images of $(ZnS)_{1-x}(MnTe)_{X,x=0.05,}$ nanophosphor. The sizes of nanoparticles are found to lie in the range 9 nm to 13 nm.This is comparable to obtained from XRD measurement.

Fig 3 show the SEM image of $(ZnS)_{1-x}(MnTe)_{X,x=0.05,}$ nanophosphor. The average grain size estimated from SEM image verifies that the phosphor sizes are in nanometer range.

Fig 4 shows the TL glow curves for $(ZnS)_{1-x}(MnTe)_X$ nanophosphor for different compositions of x. In this sample the first peak intensities lies nearly 105 °C-100 ^{0}C and second peak intensity lies nearly 183.5 ^{0}C -178.5 ^{0}C. The curves I, II, III, and IV corresponds the UV irradiation with 10 min, 25 min, 20 min, 15 min. It is seen that peak temperature first increases than decreases by increasing UV exposure time. It is seen that initially the TL intensity increases with ultraviolet exposure time and then it start decreasing with further increase in the ultraviolet exposure time. The primary resion for the decrease of the TL intensity with longer duration of UV exposure is the increase in temperature of the phosphor caused by the heat from ultraviolet lamp.

Fig 5 shows the ML response to a mechanical impact for $(ZnS)_{1-x}$ $(MnTe)_x$ phosphor. In this case, the ML was excited by dropping a load of 400 gm, in which the dropping heights were changed to different values. It is found that the ML intensity rise with the increase of the impact velocity of the load on to phosphors. It is seen that when a load of a fixed mass was dropped on to the phosphor of a given mass from a known height, then an ML pulse is produced, in which at the beginning ML intensity rises linearly with time, attains a optimum value and then it

decreases with time. The peak of the ML intensity I_m increases linearly with the impact velocity $v_o = (2gh)^{1/2}$, where g is acceleration because of gravity and h is the height from which the load was dropped. No significant changes were found in the time t_m corresponding to the peak of ML intensity versus time, with increasing value of the impact velocity v_o.

Fig.6 shows the PL spectra of $(ZnS)_{1-x}(MnTe)_{x,x=.05}$ phosphors. It is seen that the peak of the PL spectra occurs at 644 nm. For the measurement the wavelength of light used for excitation was 300 nm.

Fig. 7 Illustrates the dependence of TL and PL intensity in $(ZnS)_{1-x}(MnTe)_{x,x=.05}$ phosphors on the value of x. It is evident that the initially the ML and PL intensity increas with x, attain an optimum value for x=0.05 then they decrease with further increase in x.

Fig 8 Illustrates the dependence of ML and PL intensity in $(ZnS)_{1-x}(MnTe)_{x,x=.05}$ phosphors on the value of x.

4. DISCUSSION

. The average sizes of ZnS nanoparticles were estimated from the Debey-Scherrer formula using XRD. The size of the nanoparticles prepared at room temperature, 50, 100, and 200^0 C, were 1.81, 2.50, 2.74 and 3.01 nm, respectively.

The photoluminescence spectra emission peak was centered at 643 and 644 nm; the emission is in the red region. The peak at 643nm and 644 nm is attributed to Mn $^4T_1$ (^4G)→ ^{6} A_1 (^6S) transition. The red emission by the $(ZnS)_{1-X}(MnTe)_X$ nanophosphor is mainly due to Te impurity in addition to Mn in ZnS lattice. Thus the present work shows that present of Te helps the energy transfer from yellow (ZnS : Mn) to $(ZnS)_{1-X}(MnTe)_X$ red emitted centers. The present study indicates that these materials are good candidates for use in display in the red region.The PL (photoluminescence) ,ML (Mechanoluminescence), and TL (Thermoluminescence) intensity are optimum for x=0.05 in $(ZnS)_{1-x}(MnTe)_x$ phosphor because of the concentration quenching.

The thermoluminescence intensity I of nanoparticles can be expressed by the formula, I=-dm/dt=mnA, where m and n are the density of holes and electrons for recombination, respectively; and A is the carrier recombination probability. In fact, with increase in the content of the surface states, holes and electrons of the particle become more accessible for the TL recombination, i.e., the m and n increase proportionally with the surface states. As the surface states increases with decrease in the size of the particle, nanoparticles with smaller size causes the increase in the TL efficiency. Furthermore, the wave functions of electrons and holes are effectively overlapped in nanoparticles, and this may also cause increase in their recombination probability, A. Because of these two factors, the TL of small nanoparticles is expected to be more than that of the bulk. Fig. 8 shows the schematic diagram for the size dependence of the surface states. It is to be noted that the separation between the electron–hole states (similar to the donor–acceptor pairs) increases with the decreasing size of the nanoparticles because the trap-depth does not change much upon decreasing size, while the bandgap increases .In the case of $(ZnS)_{1-x}(MnTe)_x$ phosphors also the trap depth should not change significantly with increasing size of the nano-phosphors.

Calculation of Trap Depth and Frequency Factor

The phosphor was given a UV irradiation using UV source for 10 min, 25 min, 20 min, and 15 min. Every time 2 mg of weighted phosphor was taken for TL measurements. We have calcutaled the trapping parameters like trap depth (E) and escape frequency factor (s) for glow peaks obtained under ultraviolet excitation.

The trap depth was determined using the following eqation

$$E = \frac{2kT_m^2}{\delta} \qquad \ldots (1)$$

where E=trap depth, k= boltzman constant, T=temperature, $\delta = T_2 - T_m$, T_2 and is the temperature to higher temperature side of full- width half- maxima.

The Frequency Factor was determined using the following formula

$$s = \beta \frac{E}{T_m^2} e^{\left(\frac{E}{kT_m}\right)} \qquad \ldots (2)$$

where s= Frequency Factor, β = Heating Rate, E=trap depth, k= boltzman constant, and T_m= peak temperature,

Table 1 shows the first and second peak position of nanophosphor for different values of x. The frequency factor, activation energy of first and second peak is given in table 1

Table 1: Values of peak temperature, Activation Energy (E) and Frequency Factor (s) of first and second peak for $(ZnS)_{1-x}(MnTe)_X$ for different composition of x.

S.N.	phosphors	Ist Peak Temp (°C)	Activation Energy E1 (eV)	Frequeny Factor s_1 (sec $^{-1}$)	IInd Peak Temp (°C)	Activation energy E2 (eV)	Frequeny Factor s_2 (sec $^{-1}$)
1.	$(ZnS)_{1x}(MnTe)_{X,x=0.02}$	105	0.4636	4.9 x 10 ^{11}	183.5	0.7626	9.9 x 10 ^{13}
2.	$(ZnS)_{1x}(MnTe)_{X,x=0.05}$	104	0.4612	4.7 x 10 ^{11}	182.5	0.7592	9.5 x 10 ^{13}
3.	$(ZnS)_{1x}(MnTe)_{X,x=0.10}$	103	0.4580	4.5 x 10 ^{11}	181.5	0.7559	9.3 x 10 ^{13}
4.	$(ZnS)_{1x}(MnTe)_{X,x=0.15}$	102	0.4563	4.4 x 10 ^{11}	180.5	0.7526	8.5 x 10 ^{13}
5.	$(ZnS)_{1x}(MnTe)_{X,x=0.20}$	101	0.4539	4.2 x 10 ^{11}	179.5	0.7493	8.2 x 10 ^{13}
6.	$(ZnS)_{1x}(MnTe)_{X,x=0.25}$	100	0.4515	4.1 x 10 ^{11}	178.5	0. 7460	7.9 x 10 ^{13}

5. CONCLUSIONS

The various glow curve (TL, ML, PL) of $(ZnS)_{1-x}(MnTe)_x$ nanophosphors having average size 11 nm has been studied for various composition of x. It is found that the luminescence intensity is maximum for x=0.05. Initially the Ml ,TL,and PL, intensity increases with increasing value of x because the number of luminescence centres increases however, for higher values of x the intensity decreases because of the concentration quenching. Thus the TL, ML and PL intensities are optimum for particular value of x that is for x=0.05. The activation energy of first and second peaks for all the samples was calculated and they are found to be first 0.45 eV and second 0.75 eV, respectively. The frequency factor is also calculated of first and second peak and it was found to be in the range of 4.4 x10 ^{11} and 8.8 x 10 ^{13} sec^{-1} respectively.

REFERENCES –

[1] S.W.S. Mckveever, thermoluminescence of solids, Cambridge University press, (1988).
[2] Claudio Furetta, "Hand book of thermoluminescence" World Scientific Pub. Co. Inc. (2003).
[3] M.Oberhofer and A.Scharmann, Applied thermoluminescence dosimetry, edited by M.Oberhofer and A.Scharmann, published by adam higher Ltd. Techno house, Redchiffney, Bristel (1981).
[4] D.R.Vij, Luminescence of solids, Edited by D.R. Vij, Plennum press, New York and London (1998).
[5] Stuart James Fleming, Thermoluminescence techniques in archaeology, Clarendon Press, (1979).
[6] B.P. Chandra, V.K. Chandra, Piyush Jha, Luminescence of II-VI semiconductor nanoparticle. Sol. Stat. Phenomenon, 222 (2015) 1.
[7] P. Yang, M. Lü , D. Xü, D. Yuan and G. Zhon, Catalytic growth and photoluminescence properties of semiconductor single-crystal ZnS nanowires. Chemical Physics Lett. 336 (2001)76.
[8] R.N. Bhargava and D. Gallangher, Optical properties of manganese-doped nanocrystals of ZnS. Physical Review Letters 72(1994) 416.
[9] H. Chander, A Review on Synthesis of Nanophosphors – Future Luminescent Materials Material Science and Engineering, R49 (2005)113.
[10] X. Fang, T.Zhai, U.K.Gautum, L.Li, L.Wu, Y.Bando, D.Golberg, ZnS nanostructures: from synthesis to applications Progress in Materials Science, 56(2011)175-287.
[11] K. Manzoor, S.R. Vadera, N. Kumar, T.R.N. Kutty, Energy transfer from organic surface adsorbate-polyvinyl pyrrolidone molecules to luminescent centers in ZnS nanocrystalsSolid State Communication, 129 (2004) 469.
[12] H. Yang, S. Santra, and P.H. Holloway, Nanobiomaterials Handbook Journal of Nanoscience and Nanotechanology 5(2005)1364.
[13] Y. Yang, J.M. Huang, S.Y. Liu, J.C. Shen, Macromolecules Containing Metal and Metal-Like Elements.J.Mater.Chem. 7(1997)131.
[14] K. Manzoor, S.R. Vadera, N. Kumar, T.R.N. Kutty, Inorganic Nanoparticles: Synthesis, Applications, and Perspectives Applied Physics Letters 84(2004) 284.
[15] B.P. Chandra, C.N. Xu, H. Yamada, X.G. Zheng, Intense visible **luminescence**from Nd-doped yttrium oxysulfide. Journal of Luminescnce, 130 (2010)442.
[16] C.N. Xu, T. Watanabe, M. Akiyama, X.G. Zheng, Elastico-mechanoluminescence in
[17] CaZr(PO4)2:Eu2+ with multiple trap levels Appl.Phys.Lett. 74(1999)1236.
[18] B.P. Chandra, V. K. Chandra, Piyush Jha, Piezoelectrically-induced trap-depth reduction model of elastico-mechanoluminescent materials Physica B 461(2015) 38.
[19] W. Chen, Z. Wang, Z. Lin, and L. Lin, Advanced Material J. Appl. Phys. 82 (1997a) 3111,156-159.
[20] W. Chen, Z. Wang, Z. Lin, and L. Lin, Appl. Phys.Advanced Materials Lett. 82(1997) 3111, 156-159.
[21] M. Rao, D.R. Reddy, B.K. Reddy, C.N. Xu, Intense red mechanoluminescence from $(ZnS)_{1-x}(MnTe)_x$ Phys Lett. A 372 (2008) 4122–4126.
[22] M.Rao, R.P Vijayalakshmi, D.RReddy, B.K Reddy. EPR and susceptibility studies on (ZnS)1-x(MnTe)x powdersSpectrochimica Act. A 69 (2008) 688–691.
[23] T. Toriyi, Y. Adachi, H. Yamada,Y. Imai and C. N. Xu, Enhancement of mechanoluminescence from ZnS:Mn,Te by Wet Process Key Engg. Mat. 388(2009) 301-304.

Figure Captions

Fig. 1 XRD of $(ZnS)_{1-X}(MnTe)_{X,x=0.05.}$

Fig. 2(a,b) show the TEM image of $(ZnS)_{1-X}(MnTe)_{X,x=0.05,}$ nanophosphor.

Fig. 3 show the SEM image of $(ZnS)_{1-X}(MnTe)_{X,x=0.05,}$ nanophosphor.

Fig. 4 The TL glow curves for $(ZnS)_{1-X}(MnTe)_X$ for different composition of x. The curves I, II, III, and IV corresponds the UV irradiation with 10 min, 25 min, 20 min, 15 min.

Fig 5 Time dependence the ML intensity of $(ZnS)_{1-x}(MnTe)_x$ for various composition of x (curves I,II and III correspond to the impact velocity 98, 140, and 221cm/s respectively

Fig. 6 Photoluminescence spectra of $(ZnS)_{1-x}(MnTe)_{x\ x=.05}$ phosphors.

Fig.7 Variation of TL and PL intensity with composition x in $(ZnS)_{1-x}(MnTe)_x$.

Fig .8 Variation of ML and PL intensity with composition x in $(ZnS)_{1-x}(MnTe)_x$ .Fig. 9 A schematic model for the size dependence of surface states in semiconductor nanoparticles. (a) (b) and (c) correspond to large size, medium size and small size of nano particle.

Fig 1

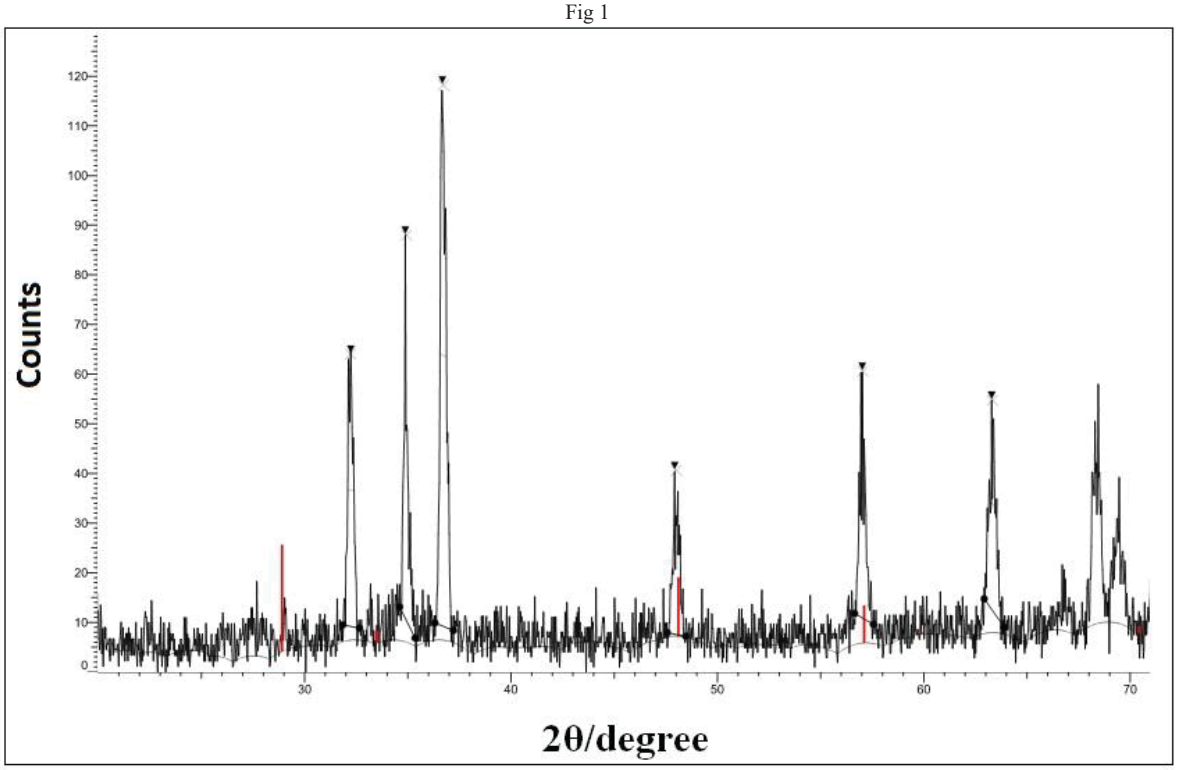
Counts
2θ/degree
0
10
20
30
40
50
60
70
80
90
100
110
120
30
40
50
60
70

Fig 2(a,b)

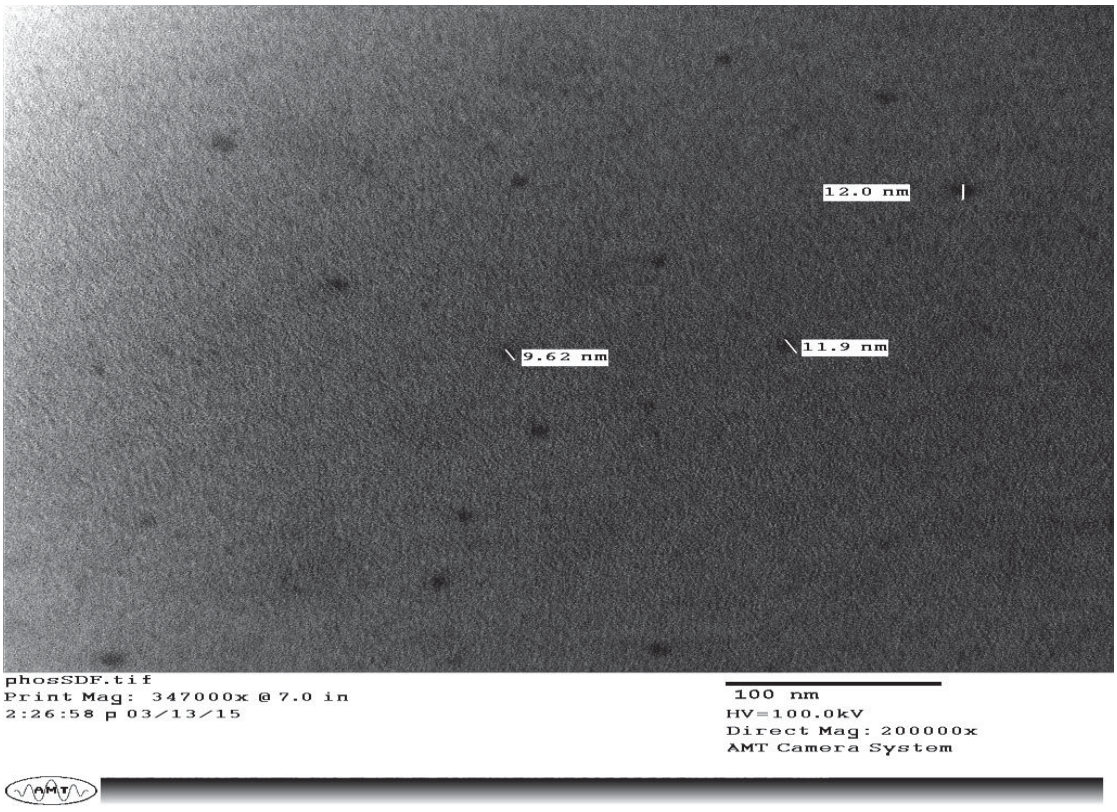
12.0 nm
9.62 nm
11.9 nm
phosSDF.tif
Print Mag: 347000x @ 7.0 in
2:26:58 p 03/13/15
100 nm
HV=100.0kV
Direct Mag: 200000x
AMT Camera System

3(a)

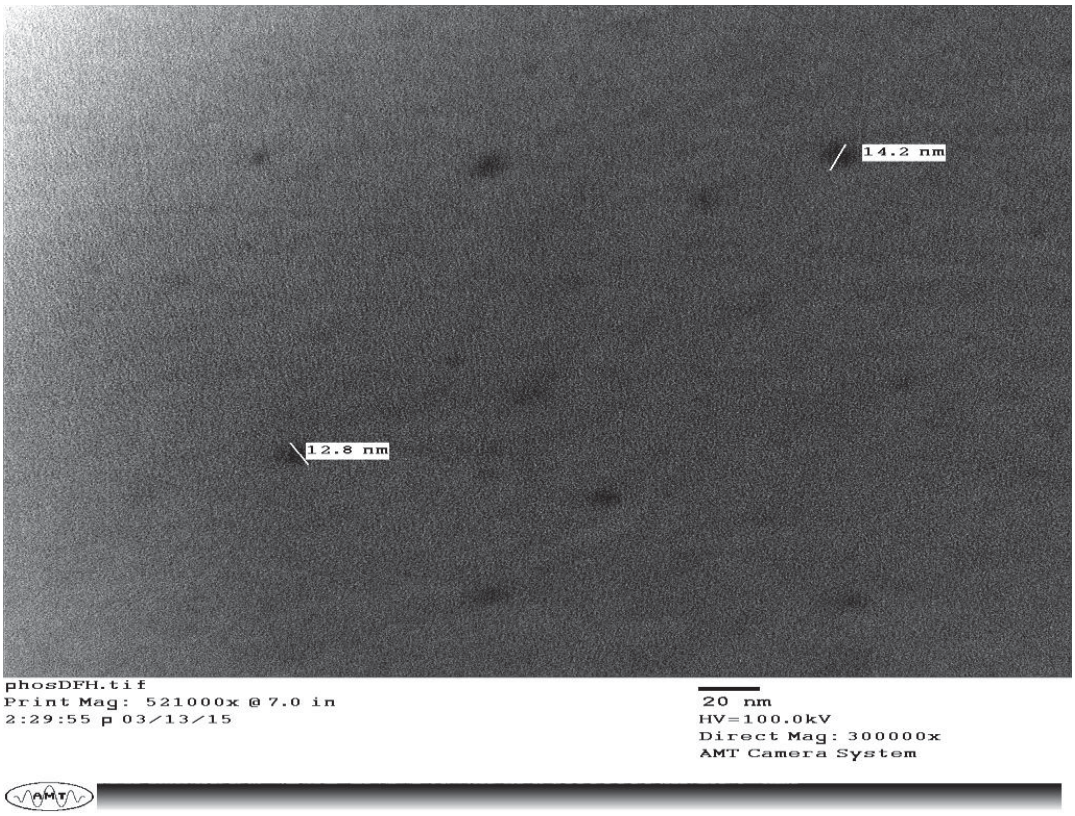
14.2 nm
12.8 nm
phosDFH.tif
Print Mag: 521000x @ 7.0 in
2:29:55 p 03/13/15
20 nm
HV=100.0kV
Direct Mag: 300000x
AMT Camera System

3(b)

Fig 3

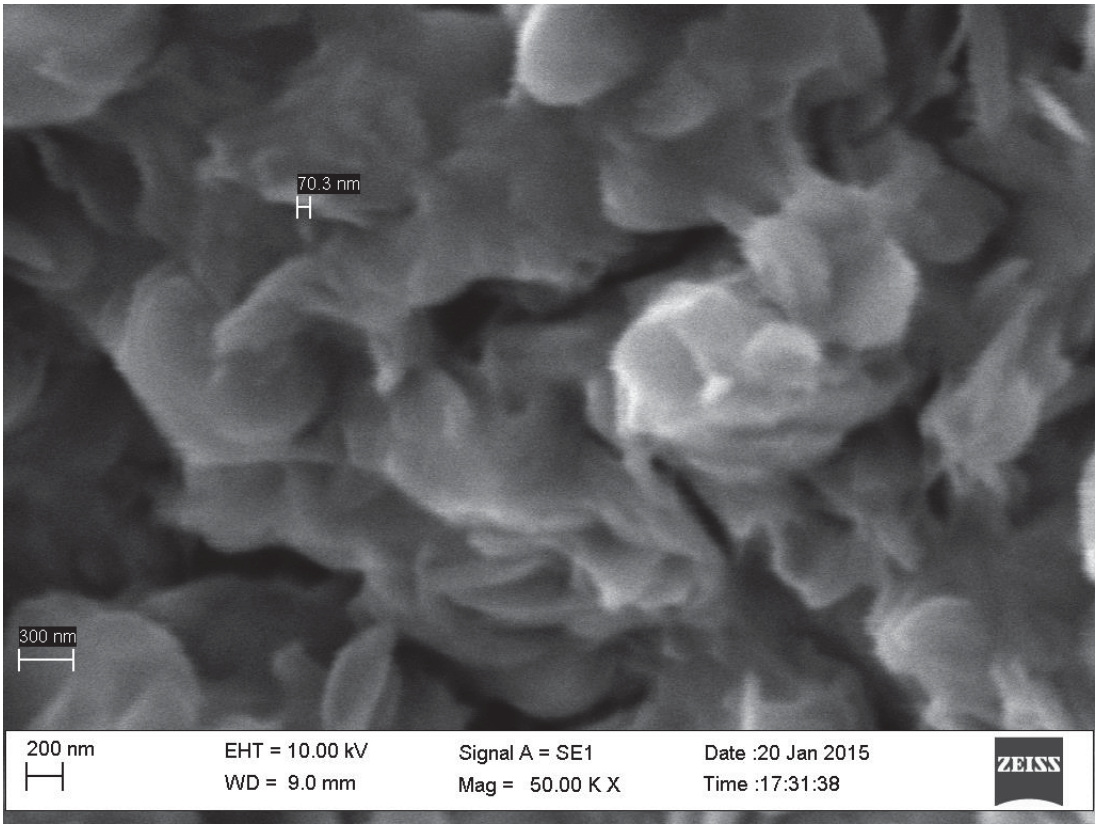
70.3 nm
300 nm
200 nm
EHT = 10.00 kV
WD = 9.0 mm
Signal A = SE1
Mag = 50.00 K X
Date :20 Jan 2015
Time :17:31:38
ZEISS

Fig :4

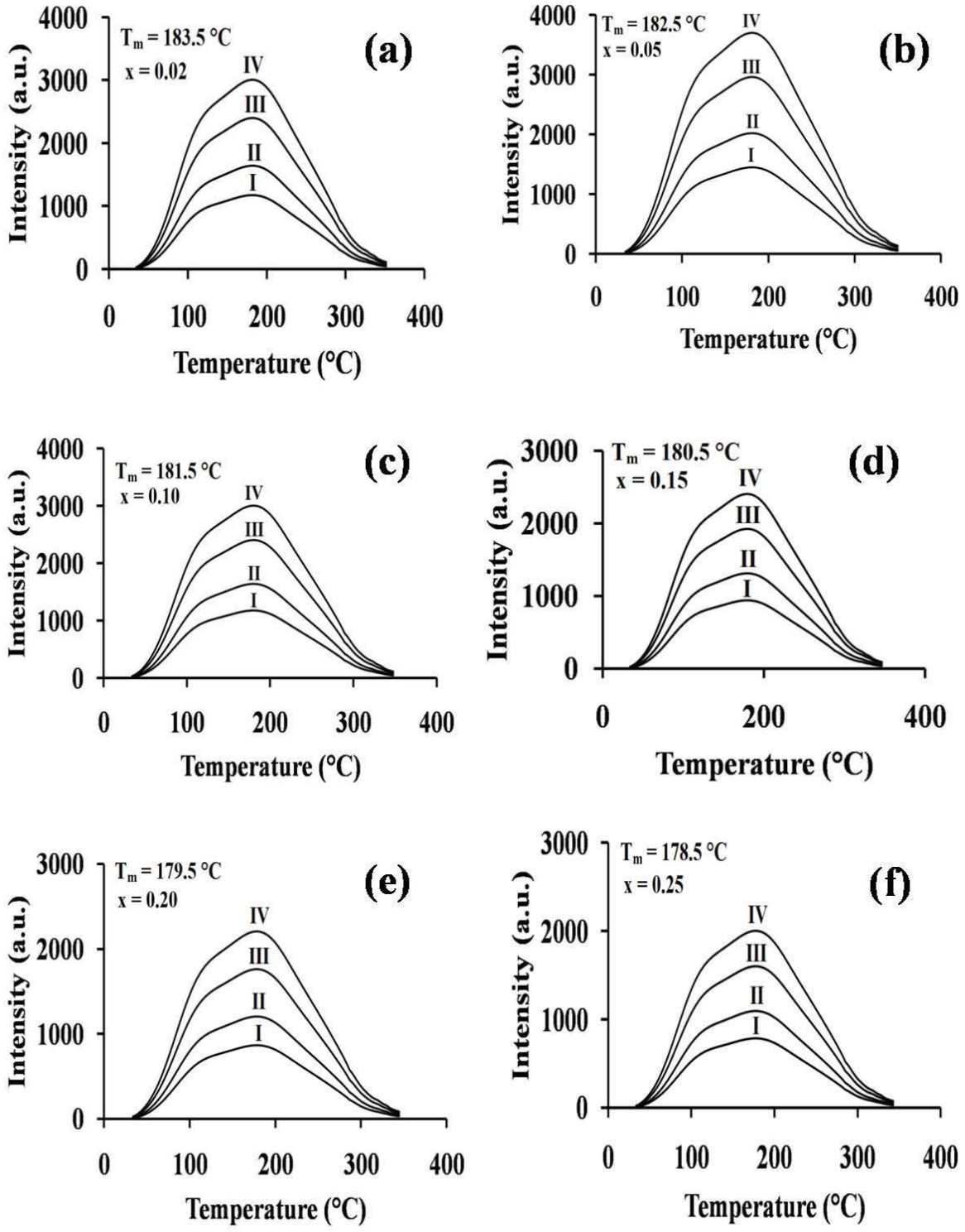
(a)
T_m = 183.5 °C
x = 0.02
(b)
T_m = 182.5 °C
x = 0.05
(c)
T_m = 181.5 °C
x = 0.10
(d)
T_m = 180.5 °C
x = 0.15
(e)
T_m = 179.5 °C
x = 0.20
(f)
T_m = 178.5 °C
x = 0.25
I
II
III
IV
Intensity (a.u.)
Temperature (°C)

Fig :5

Fig :5

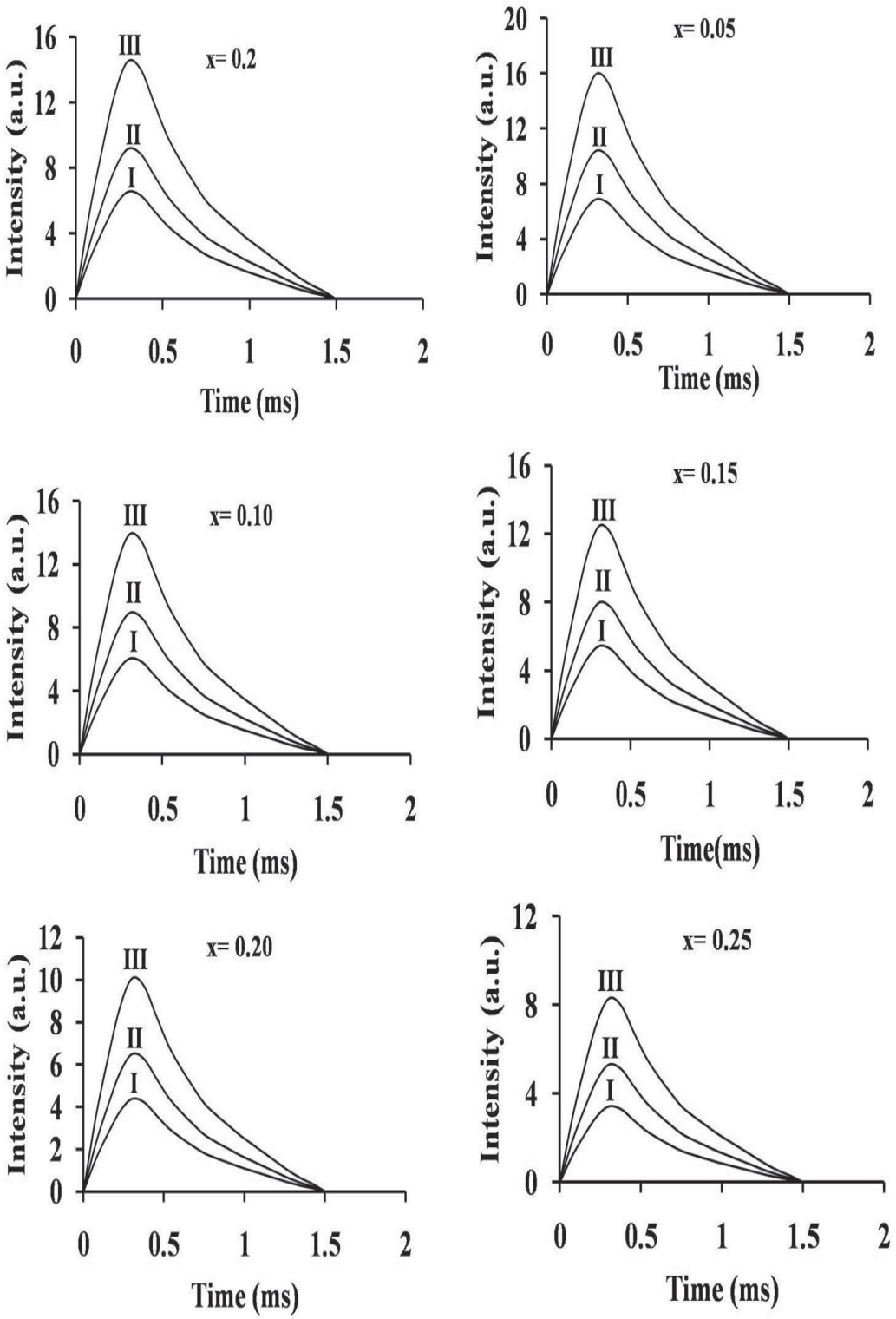
x= 0.2
x= 0.05
x= 0.10
x= 0.15
x= 0.20
x= 0.25
I
II
III
Intensity (a.u.)
Time (ms)
Time(ms)

Fig :6

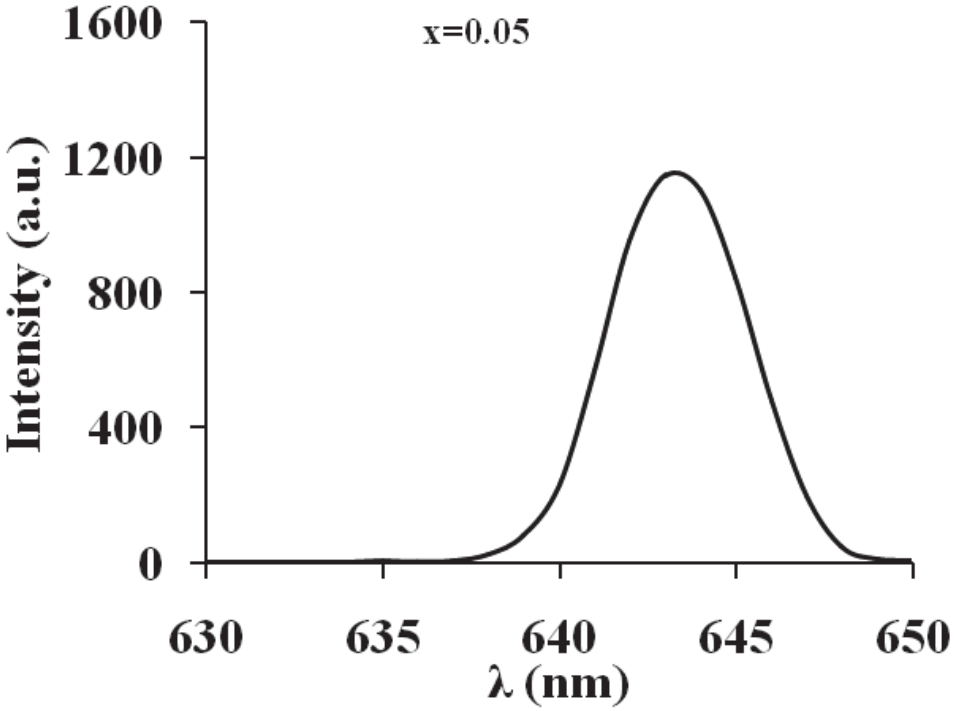
x=0.05
Intensity (a.u.)
1600
1200
800
400
0
630
635
640
645
650
λ (nm)

Fig :7

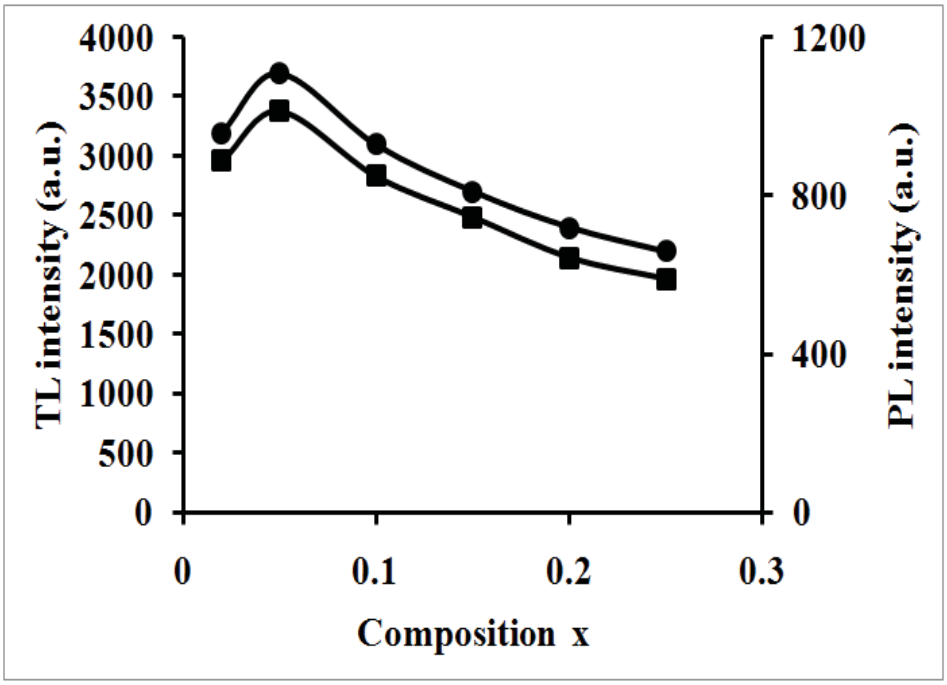
TL intensity (a.u.)
4000
3500
3000
2500
2000
1500
1000
500
0
PL intensity (a.u.)
1200
800
400
0
0
0.1
0.2
0.3
Composition x

Fig:8

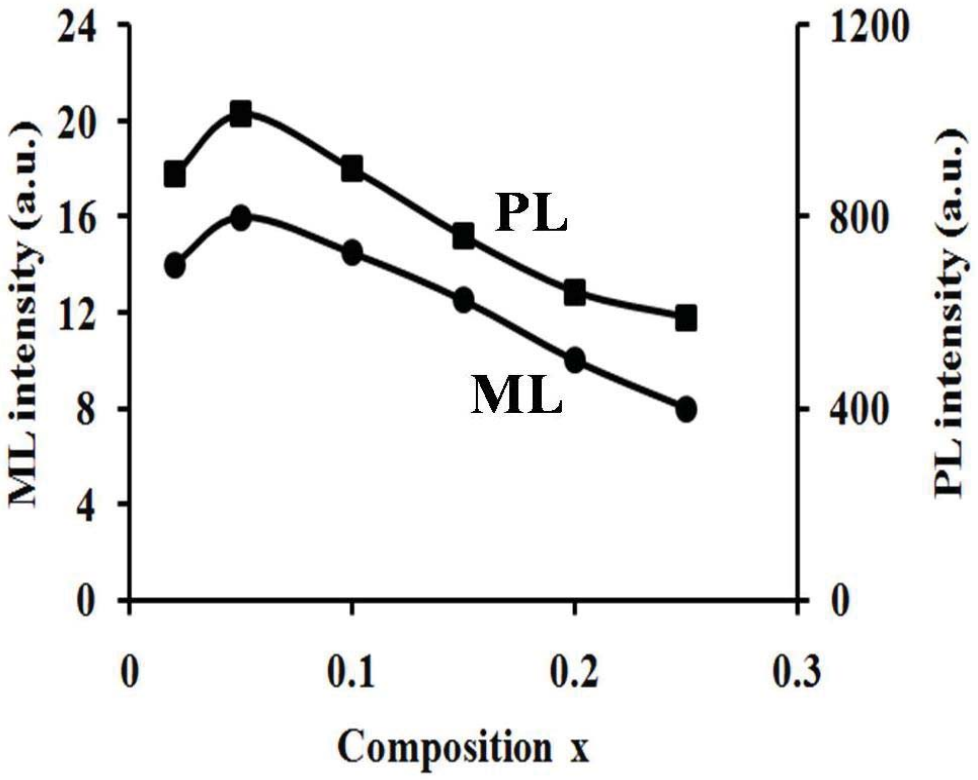
24
20
16
12
8
4
0
ML intensity (a.u.)
1200
800
400
0
PL intensity (a.u.)
PL
ML
0
0.1
0.2
0.3
Composition x

Fig: 9

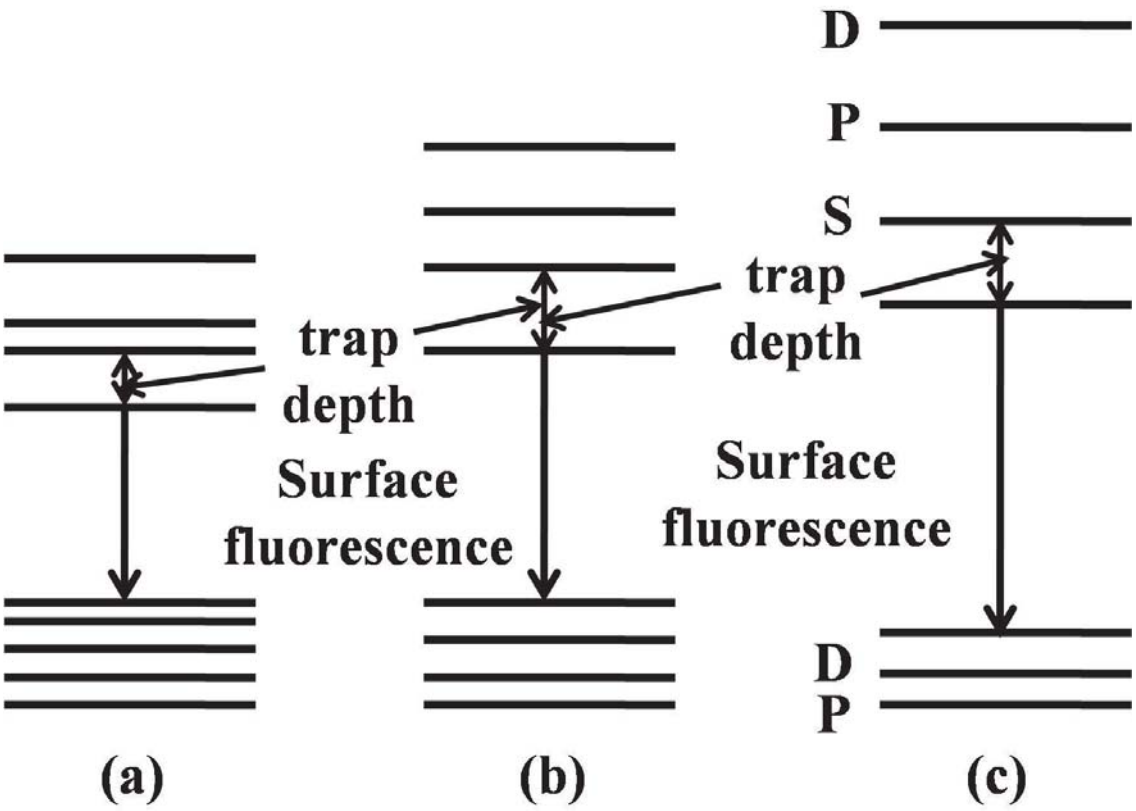
D
P
S
trap
depth
Surface
fluorescence
trap
depth
Surface
fluorescence
D
P
(a)
(b)
(c)